

# The effects of collisions on the plasma presheath

D. J. Koch and W. N. G. Hitchon

Department of Electrical and Computer Engineering, University of Wisconsin—Madison, 1415 Johnson Drive, Madison, Wisconsin 53706

(Received 21 February 1989; accepted 25 July 1989)

A numerical study of the plasma presheath has been performed, extending earlier work to include the effects of general source functions, and allowing for collisions in the presheath. Analytic results for a collisionless presheath with particular source functions have been confirmed, and comparisons with a numerical study of a weakly collisional presheath have been made. The extrapolation of these calculations to high collision frequency, where they are compared to a simple analytic model, and the effects of the choice of source functions are presented.

## I. INTRODUCTION

In this paper, a self-consistent, kinetic description of the ion distribution and the electrostatic potential  $\phi$  in a plasma presheath is presented. The calculation is applied for a wide range of collision frequencies, including the weakly collisional cases studied in the past, and a variety of source functions. Comparisons with analytic results show good agreement at both extremes of collision frequency.

The plasma presheath is a region adjacent to the sheath, with a spatial dimension  $L \gg \lambda_D$ , the Debye length, so that the presheath can be treated as quasineutral. The ratio of the mean-free path of particles  $\lambda$  and  $L/2$ ,  $\delta \equiv 2\lambda/L$ , can range from being extremely small to very large, in plasmas of practical interest.

The case  $\delta \gg 1$ , that is the collisionless case, has been studied by Emmert *et al.*<sup>1</sup> and by Bissell and Johnson,<sup>2</sup> for different choices of the source function, that is, the rate of production of ions and electrons. The electrostatic potential  $\phi$  responsible for accelerating ions into the sheath and the ion distribution function were obtained in each case. In these calculations, the sheath and its associated potential drop appear as a discontinuity because of the assumption of an infinitesimal Debye length  $\lambda_D$ .

These presheath calculations are an essential prerequisite for the equivalent calculations in the sheath, which can be considered to be collisionless in most cases of interest and as a result is easier to describe. Since edge plasmas in fusion devices and plasmas used in materials processing, for instance, are of growing interest, the extension of our capability to describe the presheath is increasingly important.

In solving the kinetic equation for the ion distribution function  $f$ , it is customary to assume that the electron density  $n_e(x)$  obeys a Boltzmann distribution. For a given ion density  $n_i(x)$ , the electrostatic potential  $\phi$  is then obtained using quasineutrality to set  $n_i = n_{e0} (e\phi/\kappa T_e)$ , where  $T_e$  is the electron temperature and other symbols have their usual meanings. This procedure will be followed here.

In this paper, the solution of the kinetic equation is obtained using a numerical scheme, which was developed for transport problems where convective transport dominates over diffusion<sup>3</sup>; the method is very efficient in this case and is somewhat more efficient than finite differences in a diffusive limit. The method, which we refer to as a "convected

scheme," utilizes a Green's function solution to a kinetic equation for the time evolution of the distribution  $f$ .

The Green's function  $p$  is essentially a probability distribution that describes the probability of a density element that is initially at  $(x_i, v_{xi})$  being at  $(x_f, v_{xf})$  after a time step  $\tau$ . The Green's function solution in the absence of collisions is given by

$$p(x, v_x, x_i, v_{xi}, \tau) = \delta \left( x - x_i - \int_0^\tau v_x dt \right) \times \delta \left( v_x - v_{xi} - \int_0^\tau a_x dt \right),$$

which is essentially a calculation of the particle trajectory in  $(x, v_x)$  phase space. Charge exchange collisions will be discussed in Sec. III.

The final distribution, after a time step  $\tau$ , is given by the convolution of the initial distribution with the Green's function:

$$f(x, v_x, t + \tau) = \int_0^L \int_{-\infty}^{\infty} p(x, v_x, x_i, v_{xi}, \tau) \times f(x_i, v_{xi}, t) dv_{xi} dx_i.$$

Details of the method and ways of obtaining the Green's function for long time steps are discussed in Ref. 3.

In the next section, the collisionless presheath is discussed and results are compared with previous analytic results.<sup>1,2</sup> Various forms of the source function  $S(x)$  are considered.

In Sec. III, the extension to a collisional presheath is done. Comparisons with the work of Scheuer and Emmert<sup>4</sup> are made and their calculations are extended to arbitrary  $\delta$ . In the very collisional limit, comparison with a simple analytic model is presented, showing good agreement. Finally, in Sec. IV, the results of this work are discussed.

## II. COLLISIONLESS PRESHEATH

A collisionless presheath is a presheath where the ions fall unimpeded through the presheath potential to the walls. For a plasma to be in steady state, a source of ions must be specified that replaces the ions that are absorbed by the walls. Two ion source functions have been examined in detail in the literature<sup>1,2</sup> and will be the basis of the computations given here.

The calculations are done in  $(x, v_x)$  phase space with perfectly absorbing walls at  $x = 0$  and  $L$  while  $v_x$  extends from  $-\infty$  to  $+\infty$ . The electrons are assumed to have a Boltzmann distribution and the motion of the ions is calculated using the convected scheme. From the ion density, the potential is found using the quasineutrality condition. Here the results of these computations will be given, for the case  $T_e = T_i = 1$  eV, and using three different ion source functions but the same total source strength.

The first ion source function to be considered was that used by Emmert *et al.*<sup>1</sup>:

$$S(x, v_x) \sim v_x \exp(-m_i v_x^2 / 2kT_i).$$

This is the density of particles, per unit of each independent variable, produced per second. The second ion source to be considered here was used by Bissell and Johnson<sup>2</sup> and Scheuer and Emmert.<sup>5</sup> It is a Maxwellian in  $v_x$  space that depends on the electron density and is given by

$$S(x, v_x) \sim n_e(x) \exp(-m_i v_x^2 / 2kT_i).$$

Both were previously used to solve the plasma equation analytically.<sup>1,2</sup>

A third source considered is a spatially uniform Maxwellian source given by

$$S(x, v_x) \sim \exp(-m_i v_x^2 / 2kT_i).$$

These ion source functions were used to calculate the steady-state potential and charge densities self-consistently.

The results of these computations and a comparison with those given by Emmert *et al.*<sup>1</sup> and Bissell and Johnson<sup>2</sup> are shown in Figs. 1 and 2, and Table I contains values of the potential at  $x = L$ . In Fig. 1, the time average potential is given for the three different source functions. The instantaneous potential can vary by as much as 10% from the time

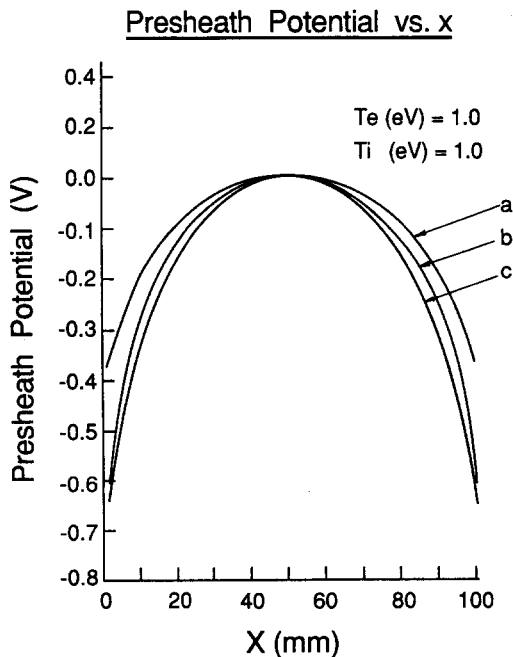
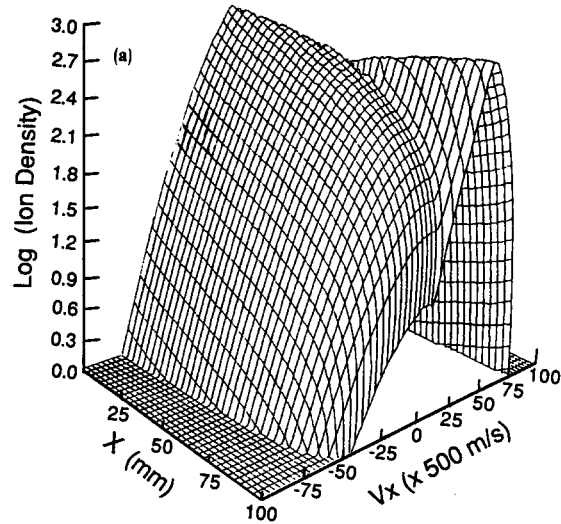


FIG. 1. Presheath potentials for different ion source functions: (a)  $\equiv$  Emmert source, (b)  $\equiv$  Bissell and Johnson source, and (c)  $\equiv$  uniform Maxwellian.

### Ion Phase Space Density

$$\begin{aligned} T_i \text{ (eV)} &= 1.0 \\ T_e \text{ (eV)} &= 1.0 \\ \delta &= \infty \end{aligned}$$



### Ion Phase Space Density

$$\begin{aligned} T_i \text{ (eV)} &= 1.0 \\ T_e \text{ (eV)} &= 1.0 \\ \delta &= \infty \end{aligned}$$

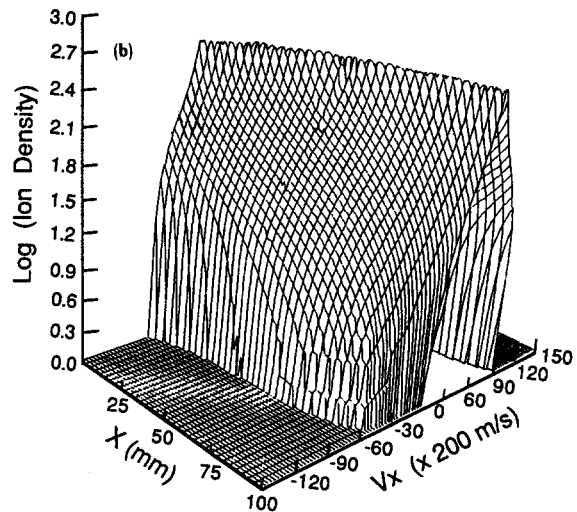


FIG. 2. Ion phase space density for (a) the Emmert<sup>1</sup> source and (b) the Bissell and Johnson<sup>2</sup> source.

average value. All potentials were estimated at the centers of the cells. Good agreement with analytic results is obtained for both the Emmert<sup>1</sup> and the Bissell and Johnson<sup>2</sup> source cases. The constant Maxwellian case had a larger ion source density at  $x = 0$  and  $L$ , which increased the difficulty of the potential calculation, and gave a slightly different presheath edge potential from that given by Bissell and Johnson.<sup>2</sup>

TABLE I. Presheath edge potentials for different sources, in the absence of collisions.

| Source type                      | Emmert <sup>1</sup> | Bissell and Johnson <sup>2</sup> | Scheuer <sup>5</sup> | This calculation |
|----------------------------------|---------------------|----------------------------------|----------------------|------------------|
| Emmert <sup>1</sup>              | − 0.4 V             | ...                              | ...                  | − 0.37 V         |
| Bissell and Johnson <sup>2</sup> | ...                 | − 0.65 V                         | − 0.624 V            | − 0.64 V         |
| Constant Maxwellian              | ...                 | ...                              | ...                  | − 0.61 V         |

Figure 2 shows the self-consistent ion phase space densities for the Emmert source [Fig. 2(a)] and Bissell and Johnson source [Fig. 2(b)] cases. These plots show the characteristics of the top three orders of magnitude of the ion phase space density. These densities are taken at the center of the mesh cell. The Emmert case has a Maxwellian distribution in velocities at the center of the plasma and the distribution is much wider in velocity space than the Maxwellian sources.

The results using a Maxwellian source show the inherent difficulty of the presheath calculations. In a numerical scheme, there is a finite spatial grid width. This width does not accurately resolve the diverging electric fields that are found in Maxwellian source cases and can introduce errors in the value of the presheath edge potential.

### III. COLLISIONAL PRESHEATH

Scheuer and Emmert<sup>4</sup> have shown that a collision mechanism such as ion-neutral charge exchange, which conserves mass but not energy or momentum has a large effect on the presheath potential. This collision process will be the focus of this study.

The calculations are done in a similar manner to those in the collisionless case. The effect of charge exchange collisions is to reduce the ion density that can travel freely along the trajectory. This is implemented by multiplying the probability distribution  $p$  by a factor of  $\exp - \{\Delta x / \lambda\}$ , where  $\Delta x$  is the distance traveled in  $x$  space during time  $\tau$ . (The distance traveled perpendicular to  $x$  is not included in the description since the perpendicular velocity is not specified, except in that collisions with the cold ions reduce the perpendicular velocity at low value.) The ions that have collided are then relaunched uniformly along the  $x$  axis between the initial and final positions of the uncollided ions with a Maxwellian distribution in the  $v_x$  direction at the neutral temperature  $T_n = 0.026$  eV. The results using the Emmert source are given in Fig. 3 for  $\infty \gg \delta \gg 0.1$  and a table of values of the potential at  $x = L$  is presented in Table II, where  $\delta = 2\lambda / L$  (an additional cell was used for the potential calculation in the Maxwellian source case). Typical ion distribution functions for the case  $\delta = 1$  are given in Figs. 4(a) and 4(b).

The method agrees with the results for the mildly collisional cases ( $\delta > 1$ ) given by Scheuer and Emmert<sup>4</sup> and gives a self-consistent solution for a strongly collisional case  $\delta = 0.1$ . The case where  $\delta = 0.1$  corresponds to conditions found in plasma processing glow discharges. As we see, the potential drop has increased by up to a factor of 3 in the most collisional case.

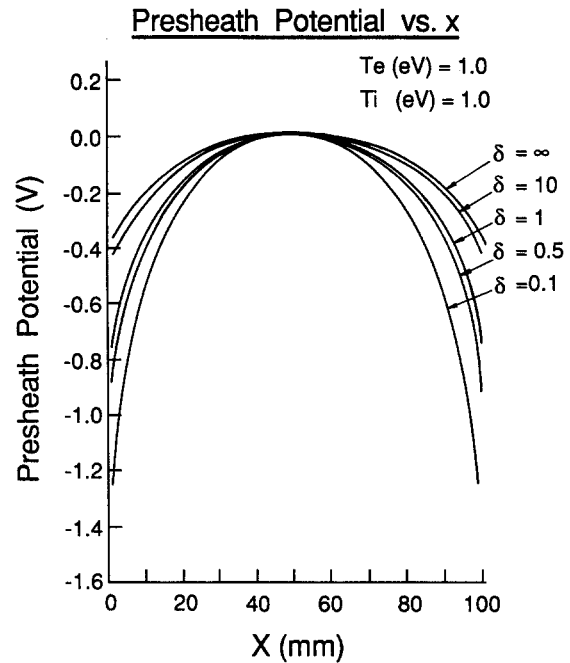


FIG. 3. Presheath potentials versus position using the Emmert source for  $\infty \gg \delta \gg 0.1$ .

The effect of collisions on the ion phase space density is to decrease the differences associated with the use of different sources [see Figs. 4(a) and 4(b)]. This is due to the increased density of scattered ions with low  $v_x$ , as shown in Fig. 4, where the scattered ion phase space density is nearly an order of magnitude higher than the unscattered density. The presheath edge potentials for different sources become virtually identical at  $\delta = 0.5$  (see Fig. 5).

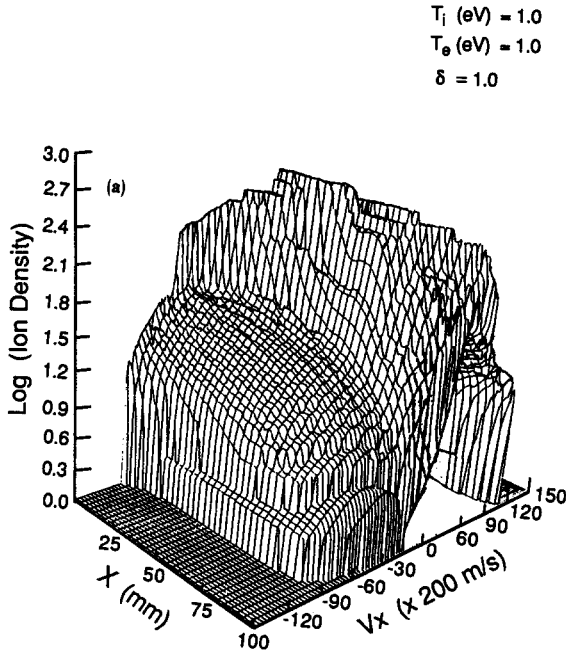
By examining Table II, we see that the errors involved in calculating the presheath potential drop increase with  $\delta$ . This is due to the singular electric field at the presheath edge that also increases with  $\delta$ . These errors can be rectified by an analysis that includes both the sheath and the presheath. This involves solving Poisson's equation, which implies having a finite  $\lambda_D$ , which will eliminate the diverging presheath electric fields. Such an analysis will be the subject of future work.

A simple kinetic theory calculation was developed for comparison with the collision dominated cases,  $\delta > 1$ . This calculation assumed that ions have a mean-free path  $\lambda$ ; the electric field is constant between collisions and the average velocity,  $\bar{v}(x) = 0.5a\bar{t}$ , where  $\bar{t}$ , the expected time between collisions, is  $\bar{t} = \{\pi\lambda / 2a\}^{1/2}$ . Using the assumption of a uniform source, the flux is given by

TABLE II. Presheath edge potentials versus  $\delta$  for the Emmert source.

| $\delta = 2\lambda / L$ | Emmert <sup>1</sup> | Scheuer <sup>4</sup> | This calculation |
|-------------------------|---------------------|----------------------|------------------|
| $\infty$                | − 0.4 V             | − 0.4 V              | − 0.375 ± 0.04 V |
| 1                       | ...                 | − 0.77 V             | − 0.76 ± 0.05 V  |
| 0.5                     | ...                 | ...                  | − 0.89 ± 0.1 V   |
| 0.1                     | ...                 | ...                  | − 1.26 ± 0.2 V   |

### Ion Phase Space Density



### Ion Phase Space Density

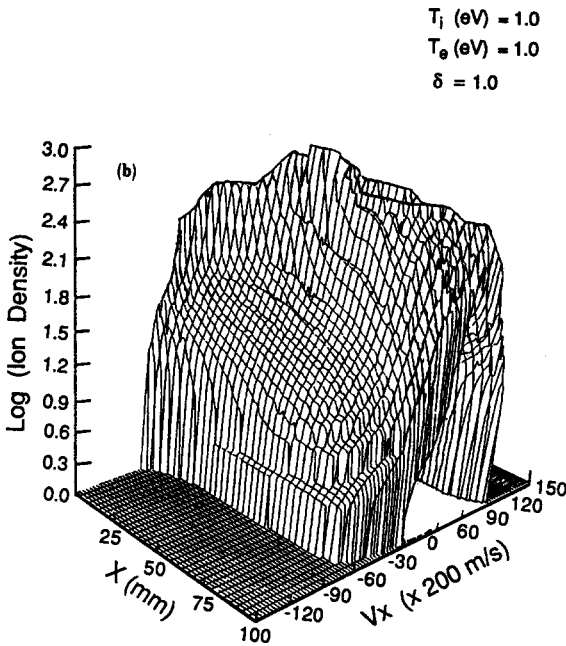


FIG. 4. Ion phase space density for  $\delta = 1$  for (a) the Emmert source and (b) the uniform Maxwellian source.

$$n_i(x)v_i(x) = S_T x,$$

where

$$S_T = \int_{-\infty}^{\infty} S dv_x.$$

This gives a relation between the ion density and the acceleration (or electric field), which is

### Presheath Potential vs. $\delta$

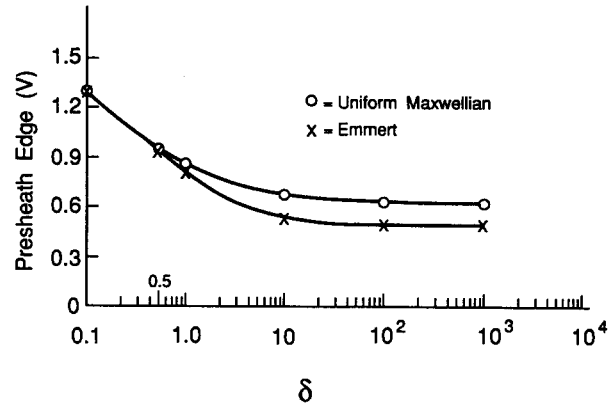


FIG. 5. Presheath potentials drop versus  $\log \delta$ ; O = uniform Maxwellian source, x = Emmert source.

$$a = 8S_T^2 x^2 / n_i^2(x) \pi \lambda.$$

The assumption of quasineutrality also gives an expression relating the potential to the charge density via the Boltzmann relation. Differentiation of the Boltzmann relation and substitution of the above expression for the acceleration give

$$\frac{dn_i^2(x)}{dx} = -\frac{16S_T^2 m_i x^2}{\lambda \pi k T_e n_i(0)}.$$

Integrating, using the boundary condition  $n_i(x) = n_i(0)$  at  $x = 0$ , gives

$$n_i^2(x) = \eta [n_i^2(0) / \eta - x^3],$$

where

$$\eta = 16m_i S_T^2 / 3\pi \lambda k T_e,$$

which is the ion density used in the analytic calculations.

The potentials, found by both methods, are given in Fig. 6 for the case  $\delta = 0.1$ . This simple approximation worked

### Presheath Potential vs. X

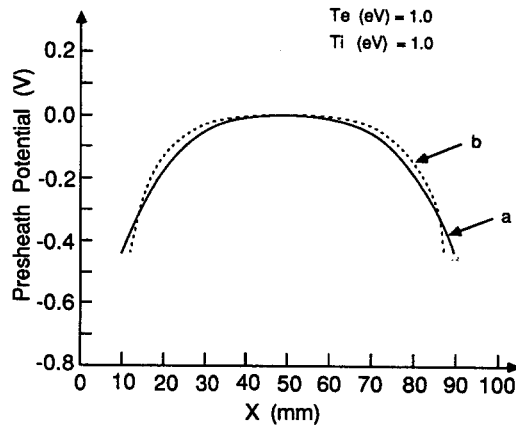


FIG. 6. Presheath potential for  $\delta = 0.1$ ; (a) = calculated using the convective scheme and (b) = using the simple kinetic model.

well at the higher collision frequencies, showing how collisions can dominate the presheath potential, as was witnessed in the ion distributions in Fig. 4. The central density used was obtained by requiring  $\phi$  to match that from the code at some location (see Fig. 6). This position is approximately the limit beyond which the analytic theory is invalid because of the assumption of a constant electric field between collisions. The value of  $n_i(0)$  found was about 20% higher than that given by the code. The curvature of  $\phi$  is small, except at the presheath edge. In the case  $\delta = 0.1$ , the curvature of  $\phi$  at the presheath edge is large enough that the quasineutrality condition begins to fail. The profiles of density and potential in the low electric field region of the presheath match reasonably well with the code. This theory predicts that the potential will vary as  $\log(\lambda^{-1/2})$ ; Fig. 5 shows the start of this dependence.

#### IV. CONCLUSION

A technique was presented that allows for the modeling of plasma presheaths for the entire range of collisionalities.

The method duplicates the results given in the literature for mildly collisional plasmas and gives self-consistent solutions at collision rates comparable to those in a glow discharge. At high collision frequency it approaches the results of a simple analytic model, which was outlined. This method can be extended to include other effects, such as those of magnetic fields on the presheath potential. Limitations resulting from diverging electric fields can be overcome by removing the assumptions of quasineutrality and infinitesimal  $\lambda_D$  and solving Poisson's equation for the potential in the sheath and presheath. These topics will be the subject of future work.

<sup>1</sup>G. A. Emmert, R. M. Wieland, A. T. Mense, and J. N. Davidson, *Phys. Fluids* **23**, 803 (1980).

<sup>2</sup>R. C. Bissell and P. C. Johnson, *Phys. Fluids* **30**, 779 (1987).

<sup>3</sup>W. N. G. Hitchon, D. J. Koch, and J. B. Adams, *J. Comput. Phys.* **83**, 79 (1989).

<sup>4</sup>J. T. Scheuer and G. A. Emmert, *Phys. Fluids* **31**, 1748 (1988).

<sup>5</sup>J. T. Scheuer and G. A. Emmert, *Phys. Fluids* **31**, 3645 (1988).



Physics of Fluids is copyrighted by the American Institute of Physics (AIP). Redistribution of journal material is subject to the AIP online journal license and/or AIP copyright. For more information, see <http://ojps.aip.org/phf/phfcr.jsp>